

Light dark matter search with CRESST-III

N. FERREIRO IACHELLINI on behalf of the CRESST COLLABORATION

Max-Planck-Institut für Physik - D-80805 München, Germany

received 17 October 2016

Summary. — The CRESST experiment uses CaWO_4 crystals operated as cryogenic detectors to search for nuclear recoil events induced by elastic scattering of dark matter particles. Results of CRESST-II have shown that a low energy threshold and the presence of light nuclei are key parameters for probing low-mass dark matter particles with high sensitivity. We present results of our last measurement campaign and how these have driven the R&D for the next CRESST-III experiment.

1. – Introduction

Many astronomical observations have shown that the mass in the Universe is largely present in the form of dark matter [1]. Despite this, today there is no observation of dark matter in particle physics. One of the most favored paradigm is the thermally produced WIMPs (Weakly Interacting Massive Particles), around which many models are centered, with predicted masses in the range of $10 \text{ GeV}/c^2$ to $1 \text{ TeV}/c^2$.

However, other approaches arose in the last years, deviating from the conventional WIMP scenario. A well motivated set of models are for instance those based on asymmetric dark matter [2]. In this picture, dark matter particles can be lighter than WIMPs, in the range of $0.1 \text{ GeV}/c^2$ to $10 \text{ GeV}/c^2$.

The CRESST-II experiment (Cryogenic Rare Event Search with Superconducting Thermometers) searches for nuclear recoil events induced by dark matter particles scattering off nuclei in CaWO_4 crystals. The experimental set-up is located at LNGS (Laboratori Nazionali del Gran Sasso), where 3400 mwe shield against cosmic radiation.

Scintillating CaWO_4 crystals are cooled down to mK temperature and are operated as cryogenic detectors [3]. An energy deposition within the crystals is mostly converted into phonons (heat), while a minor fraction ($\leq 7\%$) is re-emitted in form of scintillation photons. The phonon signal provides an accurate measurement of the deposited energy, while the simultaneous read-out of light and phonon signals offers a powerful tool to discriminate and reject electron recoils from the nuclear recoil events.

Results from CRESST-II phase 2 [4] show that a low-energy threshold and the presence of light nuclei in our targets are key for searches below $10 \text{ GeV}/c^2$.

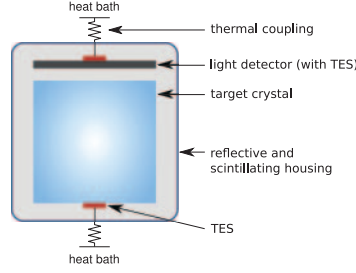


Fig. 1. – Schematic drawing of a CRESST-II detector module.

2. – Working principle of a detector module

2.1. Structure. – In CRESST-II detector modules the temperature variation of the main absorber and the emitted light are recorded simultaneously. The main absorber consists of a CaWO_4 scintillating crystal hosted in a copper housing, which offers a good thermal coupling for cryogenic operation. It is surrounded by a reflective and scintillating plastic foil. A light detector directly faces the main absorber and consists of a thin disk of either Silicon or Silicon-on-Sapphire. Both, main absorber and light detector are equipped with tungsten TES (Transition Edge Sensor) to measure temperature variations (see fig. 1).

2.2. Operation. – During cryogenic operation the detectors are kept at a temperature where the TESs are in an intermediate state between normal conduction and super conduction (fig. 2). Thanks to the steepness of the transition curve, tiny temperature variations caused by particle interactions (μK in the TES) translate into $m\Omega$ variation in the TES resistance value. The resistance change is read by a SQUID device.

2.3. Background rejection. – The simultaneous read-out of the energy deposition in the crystal and the energy converted into photons allows for background rejection. We define the Light Yield as the ratio between the energy re-emitted as scintillation light and the energy read in the phonon channel:

$$(1) \quad \text{LY} = \frac{E_{\text{light}}}{E_{\text{ph}}}.$$

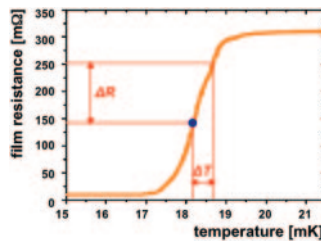


Fig. 2. – The typical shape of a transition curve is shown. By means of a heater applied onto the detector the working temperature is kept constant. A particle interaction causes a raise of the resistance value.

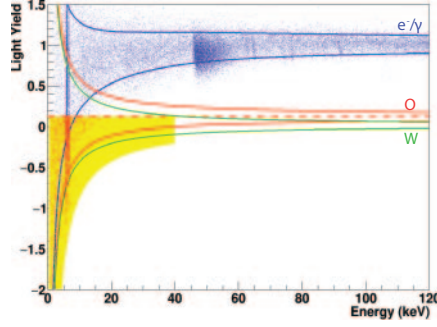


Fig. 3. – Light Yield plot of the detector Lise. Solid lines represent 90% boundaries for the recoil bands. In blue e^-/γ recoils, in red oxygen recoils and in green the tungsten recoils. The yellow box represents our acceptance region (50% of the oxygen recoils and 99.5% of tungsten recoils).

The Light Yield as a function of the energy shows a clear band structure. Electron recoils are the main source of background and they have a larger Light Yield with respect to nuclear recoils, where the sought for dark matter particles interactions are expected to appear.

2.4. Exclusion limit. – For our analysis we have considered all the events present in the yellow box in fig. 3 as potential signal events. This is a conservative choice as long as we look for an exclusion limit. In fig. 4 the exclusion we calculated is reported together with the ones of other direct dark matter searches.

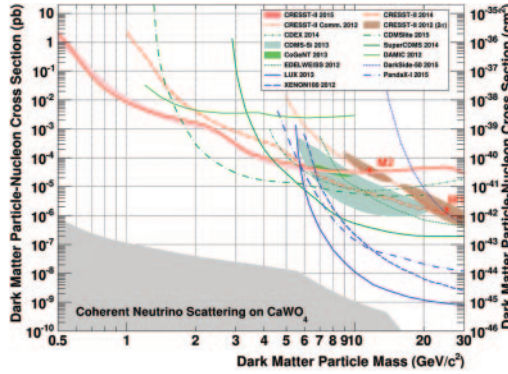


Fig. 4. – Parameter space for elastic spin-independent dark matter-nucleon scattering. The solid red line represents the exclusion obtained with detector Lise. 1σ confidence level is highlighted in light red. Other red lines are the previous CRESST-II limits [7,8]. Favored parameter space from CRESST-II phase 1 [9], CDMS-Si [10] and CoGeNT [11] are drawn as shaded areas. Exclusion with 90% CL from liquid nobles gas experiments are reported in blue [12-14]. Germanium and Silicon based experiments are reported in black [15-19]. The grey area is the solar neutrino floor [20].

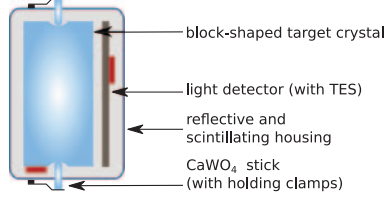


Fig. 5. – Schematic of a CRESST-III detector module. Reducing the mass of the absorber leads to a lower energy threshold. The crystal is held in its position by CaWO_4 sticks in order to veto surface background [5].

3. – Results from one CRESST-II module

Among all the detectors operated in CRESST-II we present here the one with the lowest energy threshold. Detector Lise (303 g) has a gross exposure of 52.2 kg days and the energy threshold set to 0.3 keV. A small fraction of the data (insignificant for dark matter analysis) is used as a training set to define data selection and analysis methods. Then we apply them to the entire dataset (training set excluded) blindly in order not to introduce any bias in the analysis. The Light Yield plot for detector Lise is shown in fig. 3.

3.1. Sensitivity to low masses. – From fig. 4 it is clear that liquid noble gas experiments have the highest sensitivity for dark matter particles of masses above $\sim 6 \text{ GeV}/c^2$. The region of the parameter space with masses below $6 \text{ GeV}/c^2$ is, on the contrary, better explored by cryogenic experiments. This can be explained comparing exposures and energy threshold. Liquid noble gas experiments have much larger exposures, but higher energy thresholds with respect to cryogenic experiments. A low energy threshold is the key parameter to detect low energetic nuclear recoils, induced by light dark matter particles.

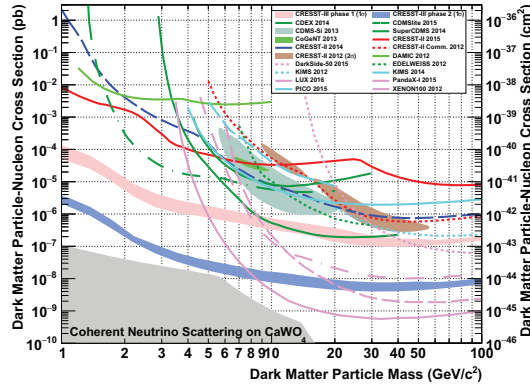


Fig. 6. – Simulated sensitivity for the upcoming CRESST-III phase 1 is reported in pink (50 kg days, 1σ CL). The future phase 2 will use 100 crystals of the type phase 1 with a reduced background by a factor 100 (light blue, 1000 kg days, 1σ CL).

4. – The new CRESST-III

Following the results of our last measuring campaign we decided to further improve our sensitivity to dark matter particles in the yet not well explored low-mass region of the parameter space. For doing so, an extensive R&D activity has been carried out which culminated in a first prototype. This first module was successfully measured underground and we have produced ten more which are currently under installation. CRESST-III phase 1 is expected to start data taking in mid-2016.

4.1. Concept. – The idea we have followed to increase the sensitivity to light dark matter particles was to further decrease the energy threshold of our detectors. To achieve this, we have reduced the mass of the main absorber to ~ 24 g and redesigned our temperature sensors. In addition we have used crystals produced at Technische Universität München, proven to have lower radioactive contamination than commercially available ones [6]. In fig. 5 the new design is drawn. The prototype of such detector has achieved an energy threshold of $O(100\text{ eV})$.

4.2. Projections. – CRESST-III will consist of ten modules as depicted in fig. 5. Assuming one year of data taking with crystals of quality as in [6] we can calculate the projection for our sensitivity. We also foresee a CRESST-III phase 2 implementing 100 CRESST-III modules and an overall background reduction of a factor 100, driven by the production within the collaboration. Both projections are reported in fig. 6.

REFERENCES

- [1] PLANCK COLLABORATION (ADE P. A. R.) *et al.*, arXiv:1303.5076 (2014).
- [2] PETRAKI K. and VOLKAS R. R., *Int. J. Mod. Phys. A*, **28** (2013) 1330028, arXiv:1305.4939.
- [3] CRESST COLLABORATION (ANGLOHER G. *et al.*), *Astropart. Phys.*, **23** (2005) 325, arXiv:astro-ph/0408006.
- [4] CRESST COLLABORATION (ANGLOHER G. *et al.*), *Eur. Phys. J. C*, **76** (2016) 25, arXiv:1509.01515.
- [5] CRESST COLLABORATION (STRAUSS R. *et al.*), *Eur. Phys. J. C*, **75** (2015) 352, arXiv:1410.1753.
- [6] CRESST COLLABORATION (STRAUSS R. *et al.*), *JCAP*, **06** (2015) 030, arXiv:1410.4188.
- [7] CRESST COLLABORATION (ANGLOHER G. *et al.*), *Eur. Phys. J. C*, **74** (2014) 3184, arXiv:1407.3146.
- [8] BROWN A., HENRY S., KRAUS H. and McCAB C., *Phys. Rev. D*, **85** (2012) 021301, arXiv:1109.2589.
- [9] CRESST COLLABORATION (ANGLOHER G. *et al.*), *Eur. Phys. J. C*, **72** (2012) 1971, arXiv:1109.0702.
- [10] CDMS COLLABORATION (AGNESE R. *et al.*), *Phys. Rev. Lett.*, **111** (2013) 251301, arXiv:1304.4279.
- [11] CoGENT COLLABORATION (AALSETH C. E. *et al.*), *Phys. Rev. D*, **88** (2013) 012002, arXiv:1208.5737.
- [12] DARKSIDE COLLABORATION (AGNES P. *et al.*), *Phys. Lett. B*, **743** (2015) 456, arXiv:1410.0653.
- [13] LUX COLLABORATION (AKERIB D. S. *et al.*), *Phys. Rev. Lett.*, **112** (2014) 091303, arXiv:1310.8214.
- [14] XENON100 COLLABORATION (APRILE E. *et al.*), *Phys. Rev. Lett.*, **109** (2012) 181301, arXiv:1207.5988.
- [15] CDEX COLLABORATION (YUE Q. *et al.*), *Phys. Rev. D*, **90** (2014) 091701, arXiv:1404.4946.

- [16] SUPERCDMS COLLABORATION (AGNESE R. *et al.*), *Phys. Rev. Lett.*, **116** (2016) 071301, arXiv:1509.02448.
- [17] SUPERCDMS COLLABORATION (AGNESE R. *et al.*), *Phys. Rev. Lett.*, **112** (2014) 241302, arXiv:1402.7137.
- [18] BARRETO J. *et al.*, *Phys. Lett. B*, **711** (2012) 264, arXiv:1105.5191.
- [19] EDELWEISS COLLABORATION (ARMENGAUD E. *et al.*), *Phys. Rev. D*, **86** (2012) 051701, arXiv:1207.1815.
- [20] GÜTLEIN A. *et al.*, *Astropart. Phys.*, **69** (2015) 44, arXiv:1408.2357.